Research Article

Functional characterization of tobacco (*Nicotiana benthamiana*) serotonin *N*-acetyltransferases (*NbSNAT1* and *NbSNAT2*)

Hyoung Yool Lee, Ok Jin Hwang, Kyoungwhan Back*

Department of Biotechnology, College of Agriculture and Life Sciences, Chonnam National University, Gwangju 61186, Republic of Korea
*Correspondence: kback@chonnam.ac.kr, Tel: +82-62-530-2165

Running title: Functional analysis of tobacco *SNAT* genes

Received: September 5, 2021; Accepted: December 4, 2021

ABSTRACT

Nicotiana benthamiana (tobacco) is an important dicotyledonous model plant; however, no serotonin *N*-acetyltransferases (SNATs) have been characterized in tobacco. In this study, we identified, cloned, and characterized the enzyme kinetics of two *SNAT* genes from *N. benthamiana*, *NbSNAT1* and *NbSNAT2*. The substrate affinity (K_m) and maximum reaction rate (V_{max}) for NbSNAT1 were 579 μM and 136 pkat/mg protein for serotonin, and 945 μM and 298 pkat/mg protein for 5-methoxytryptamine, respectively. Similarly, the K_m and V_{max} values for NbSNAT2 were 326 μM and 26 pkat/mg protein for serotonin, and 872 μM and 92 pkat/mg protein for 5-methoxytryptamine, respectively. Moreover, we found that NbSNAT1 and NbSNAT2 localized to chloroplasts, similar to SNAT proteins from other plant species. The activities of the NbSNAT proteins were not affected by melatonin feedback inhibition *in vitro*. Finally, transgenic tobacco plants overexpressing either *NbSNAT1* or *NbSNAT2* did not exhibit increased melatonin levels, possibly due to the expression of catabolic enzymes. Generating transgenic tobacco plants with downregulated *NbSNAT* expression would provide further insight into the functional role of melatonin in tobacco plants.

Key words: melatonin, *N*-acetylserotonin, 5-methoxytryptamine, serotonin *N*-acetyltransferase (SNAT), tobacco.

---

1. INTRODUCTION

N-acetyl-5-methoxytryptamine (melatonin) is a multifunctional biomolecule that is produced by photoautotrophs such as plants and even cyanobacteria, the evolutionary precursors of chloroplasts (1). Evidence suggests that the primary function of melatonin in plants is to act as a potent antioxidant, which modulates cellular redox following exposure to environmental stresses such as cold and drought (2). In addition, melatonin functions as a signaling molecule under stressful conditions, as well as during growth and development of plants (3-5). Notably, melatonin maintains and protects the integrity of two important organelles, chloroplasts and the endoplasmic reticulum (ER), by regulating chloroplast protein quality and preserving the ER structure by enhancing its secretory protein folding capacity (6, 7). Due to the multiple roles played by melatonin in plants, melatonin-deficient rice undergoes premature senescence and propagation lesion mimic phenotypes (8-10).

Melatonin is synthesized from tryptophan by four consecutive enzymes (5); serotonin *N*-

acetyltransferase (SNAT) is the penultimate enzyme in the melatonin pathway, which converts serotonin into *N*-acetylserotonin (NAS). Plant *SNAT* genes belong to the GCN5-related *N*-acetyltransferase family and can accept various substrates such as proteins and arylalkylamines (11). Two *SNAT* isogenes that have been identified and characterized in various plant species such as rice (12, 13) and arabidopsis (14, 15) play important roles in melatonin biosynthesis (16-18). Although *SNAT* genes have been functionally cloned from several plant species, no information is available regarding *SNAT* genes in *Nicotiana benthamiana* (tobacco). Tobacco is an important dicotyledonous model plant because of its easy genetic transformation. Although arabidopsis is a good model plant, it produces low melatonin with about 50 pg/g fresh weight which is unable to be detected by HPLC. In order to find the best dicotyledonous model plant which produces more melatonin than arabidopsis which in turn enables us to easily detect melatonin by HPLC, here we employed tobacco. In this study, we identified and cloned two *SNAT* genes from tobacco, and enzymatically characterized the recombinant SNAT proteins. Furthermore, we generated transgenic tobacco *SNAT* overexpression lines, and found that their melatonin levels did not differ significantly from the wild type, suggesting that melatonin is rapidly catabolized in tobacco plants.

2. MATERIALS AND METHODS

2.1. Vector construction and *Escherichia coli* expression.

Full-length tobacco *NbSNAT1* and *NbSNAT2* cDNAs were generated by reverse transcription-polymerase chain reaction (RT-PCR) using total RNA isolated from 2-week-old tobacco leaves and a specific primer set, which was designed using sequence information deposited in the Solanaceae Genomics database (19). The resulting PCR products were each cloned into a T&A cloning vector (RBC Bioscience, New Taipei City, Taiwan) to generate vectors T&A-NbSNAT1 and T&A-NbSNAT2, whose sequences were confirmed via sequencing (Bioneer, Daejeon, Korea). *NbSNAT1* and *NbSNAT2* cDNA fragments lacking transit sequences were further amplified by PCR using primers with attB recombination sequences (*NbSNAT1* forward primer, 5´-GGG GAC AAG TTT GTA CAA AAA AGC AGG CTC CAT GGT TAT AGA ATC AC-3´; *NbSNAT1* reverse primer, 5´-GGG GAC CAC TTT GTA CAA GAA AGC TGG GTT TAA TAC ATT GGA TAC CA-3´; *NbSNAT2* forward primer, 5´-GGG GAC AAG TTT GTA CAA AAA AGC AGG CTC CAT GGT AAA CAT CTC AA-3´; *NbSNAT2* reverse primer, 5´-GGG GAC CAC TTT GTA CAA GAA AGC TGG GTT CAC CTA TTC TTT TTC TTT TTC CT-3´). The resulting PCR products were gel purified and cloned into the pDONR221 Gateway® vector (Invitrogen, Carlsbad, CA, USA) via BP recombination between the *attB*-flanked PCR product and the donor vector containing *attP* sites, which created an entry clone. The pDONR221:Δ78NbSNAT1 and pDONR221:Δ39NbSNAT2 gene entry vectors were then recombined with the pET300 Gateway destination vector via LR recombination to form the pET300-Δ78NbSNAT1 and pET300-Δ39NbSNAT2 vectors. To generate pET28b-Δ78NbSNAT1 and pET22b-Δ39NbSNAT2, specific primers containing *Nde*I and *Xho*I restriction sites were used to amplify the inserts via PCR; the PCR products were digested with *Nde*I/*Xho*I restriction enzymes and subcloned into pET28b or pET22b vectors (Invitrogen) predigested with the same restriction enzymes. All plasmids were transformed into *E. coli* strain BL21(DE3).

2.2. Purification of recombinant NbSNAT1 and NbSNAT2.

First, 10 mL of *E. coli* overnight cultures containing *NbSNAT1* and *NbSNAT2* expression vectors were inoculated into 100 mL of Terrific Broth (20 g/L Bacto-tryptone, 24 g/L Bacto-

yeast extract, 4 mL/L glycerol, and phosphate buffer [0.017 M monopotassium phosphate and 0.072 M dipotassium phosphate]) supplemented with 50 mg/L ampicillin or 50 mg/L kanamycin (pET28b-Δ78NbSNAT1) and incubated at 37°C until the optical density at 600 nm reached 1.0. After the addition of isopropyl-β-D-thiogalactopyranoside (Sigma, St. Louis, MO, USA) up to 1 mM, the culture was grown at 28°C with shaking at 180 rpm for 5 h. The protein was purified via affinity nickel ion chromatography according to the column manufacturer's instructions (Qiagen, Tokyo, Japan).

2.3. Measurement of SNAT enzyme activity.

Purified recombinant SNAT was incubated in 100 µL of 100 mM potassium phosphate (pH 8.8 or various pH values) containing 0.5 mM serotonin and 0.5 mM acetyl-coenzyme A. All SNAT enzyme assays were conducted at 45 °C for 30 min (or various temperatures) and stopped by adding 25 µL of methanol. Then, 10 µL aliquots of the reaction mixture were subjected to high-performance liquid chromatography (HPLC) coupled to a fluorescence detector system as described previously (14, 20). Non-enzymatic reaction products that were generated in the absence of the SNAT enzymes were discounted. To determine substrate affinity (K_m) and maximum reaction rate (V_{max}), we applied various substrates and enzyme concentrations. The K_m and V_{max} values were calculated using Lineweaver–Burk plots. Protein concentration was determined using Bradford assays (Bio-Rad, Hercules, CA, USA). The analyses were performed in triplicate.

2.4. Subcellular localization of NbSNAT1 and NbSNAT2.

The pER-mCherry vector was kindly donated by Dr. H. Kang (Texas State University, USA). Full-length *NbSNAT1* and *NbSNAT2* cDNA were each cloned into the binary pER8-mCherry vector at the *Asc*I restriction sites downstream of the estrogen-inducible XVE promoter to generate NbSNAT1-mCherry and NbSNAT2-mCherry fusion proteins. The plasmids were transformed into *Agrobacterium tumefaciens* strain GV2260 using the freeze–thaw method. Then, transient expression analyses were performed as described previously (20). Briefly, two-week-old *N. benthamiana* leaves were infiltrated with *A. tumefaciens* strain GV2260 carrying pER8:NbSNAT1-mCherry or pER8:NbSNAT2-mCherry plasmids. The transformed tobacco leaves were then examined using confocal microscopy to determine the subcellular localization of the NbSNAT fusion proteins. β-estradiol (Sigma Aldrich, St. Louis, MO, USA) treatment and confocal microscopy were performed as described previously (20).

2.5. Transgenic tobacco plants overexpressing *NbSNAT1* and *NbSNAT2*.

Full-length *NbSNAT1* and *NbSNAT2* PCR products were gel purified and cloned into the pDONR221 Gateway vector (Invitrogen) via BP recombination. The resulting pDONR221:NbSNAT1 and pDONR221:NbSNAT2 entry vectors were then recombined with the pK2GW7 Gate destination vector (21) via LR recombination to form the pK2GW7-NbSNAT1 and pK2GW7-NbSNAT2 vectors, which were transformed into *A. tumefaciens* GV2260. Tobacco transformation was carried out according to Duan *et al.* (22). Briefly, sterile *N. benthamiana* leaf disks were incubated with *Agrobacterium* strains and 100 µM acetosyringone, and then incubated at 25°C in the dark for 3 days. After co-cultivation, the explants were transferred to Murashige and Skoog (MS) medium containing 4.44 µM 6-benzylaminopurine, 0.57 µM indole-3-acetic acid, 3% sucrose, 50 mg/L kanamycin, and 250 mg/L timentin, and then incubated for 6–8 weeks at 25 °C under a 12 h light/12 h dark cycle. After obtaining T_1 seeds, only single copy insertion lines (T_1) showing a 3:1 segregation ratio

for kanamycin resistance (200 mg/L) were selected and further selfed for T_2 seeds. The T_2 homozygous lines that all seeds exhibit kanamycin resistance were used for further analyses.

2.6. Melatonin quantification.

Melatonin levels were quantified via HPLC as described previously (23). In brief, melatonin was extracted from 0.1 g of tobacco leaves using 1 mL of chloroform; the suspension was centrifuged for 10 min at 13500 × *g* at room temperature. The chloroform fractions were evaporated, and the remaining precipitate dissolved in 0.2 mL of 40% methanol. Aliquots (20 µL) were analyzed using a HPLC machine equipped with a fluorescence detector (2475; Waters, Milford, MA, USA). The samples were separated using a Sunfire C18 column (4.5 × 150 mm; Waters, Milford, MA, USA) with a gradient elution profile of 42–50% methanol in 0.1% formic acid for 27 min, followed by 18 min of isocratic elution with 50% methanol in 0.1% formic acid at a flow rate of 0.15 mL/min. Melatonin was detected using excitation and emission wavelengths of 280 nm and 348 nm, respectively. All measurements were performed in triplicate.

2.7. Reverse transcription-polymerase chain reaction (RT-PCR) analysis.

To estimate the mRNA expression levels of the *NbSNAT* genes in the transgenic tobacco plants, we performed RT-PCR. Total RNA was isolated from *N. benthamiana* leaves using a NucleoSpin RNA Plant Kit (Macherey-Nagel, Düren, Germany). First-strand cDNA was synthesized from 2 µg of total RNA using MG MMLV Reverse Transcriptase (MGmed, Inc., Seoul, South Korea) and an oligo dT_{18} primer at 42°C for 1 h. RT-PCR was performed using the following primer set: *NbSNAT1* forward 5’- GTT ATA GAA TCA CCA-3’, *NbSNAT1* reverse 5’-ATT GAA AGC ATG ATC TGA-3’, *NbSNAT2* forward 5’-GTA AAC ATC TCA ATC TCC-3’, *NbSNAT2* reverse 5’-AG CTG GGT GAC TAA TCT TTC CAT CAC-3’, *18s RNA* forward 5'-AGG ATT GAC AGA CTG AGA GC-3', and *18s RNA* reverse 5’-AG CTG GGT GAC TAA TCT TTC CAT CAC-3’. The PCR was performed as previously described (24).

2.8. Statistical analysis.

Data were compared using analysis of variance followed by post-hoc Tukey’s honest significant difference tests. Statistical analyses were performed using SPSS Statistics software (ver. 25.0; IBM Corp., Armonk, NY, USA). *P*-values < 0.05 were considered to indicate statistical significance.

3. RESULTS

3.1. Identification of tobacco *SNAT* isogenes.

To identify *SNAT* genes in *N. benthamiana*, database searches were performed using the *Oryza sativa* (rice) *SNAT1* (*OsSNAT1*) and *SNAT*2 (*OsSNAT2*) gene sequences as queries to screen the *N. benthamiana* genome. Using an amino acid BLAST search, the two *SNAT* isogenes were identified in the *N. benthamiana* genome (19). NbSNAT1 (Accession number: Niben101Scf09906g02025.1) shared 72% sequence identity with the OsSNAT1 mature polypeptide, while NbSNAT2 (Accession number: Niben101Scf10613g00009.1) shared 54% sequence identity with the OsSNAT2 mature polypeptide (Figure 1). The *NbSNAT1* and *NbSNAT2* genes were 771 bp and 582 bp long and encoded 256 and 193 amino acids,

respectively. Similar to the *OsSNAT* isogenes, N-terminal chloroplast transit sequences with lengths of 78 and 39 amino acids were predicted using TargetP in NbSNAT1 and NbSNAT2 (25). Full-length cDNA for *NbSNAT1* and *NbSNAT2* was cloned via RT-PCR using RNA isolated from tobacco leaves and then verified by sequencing analysis.

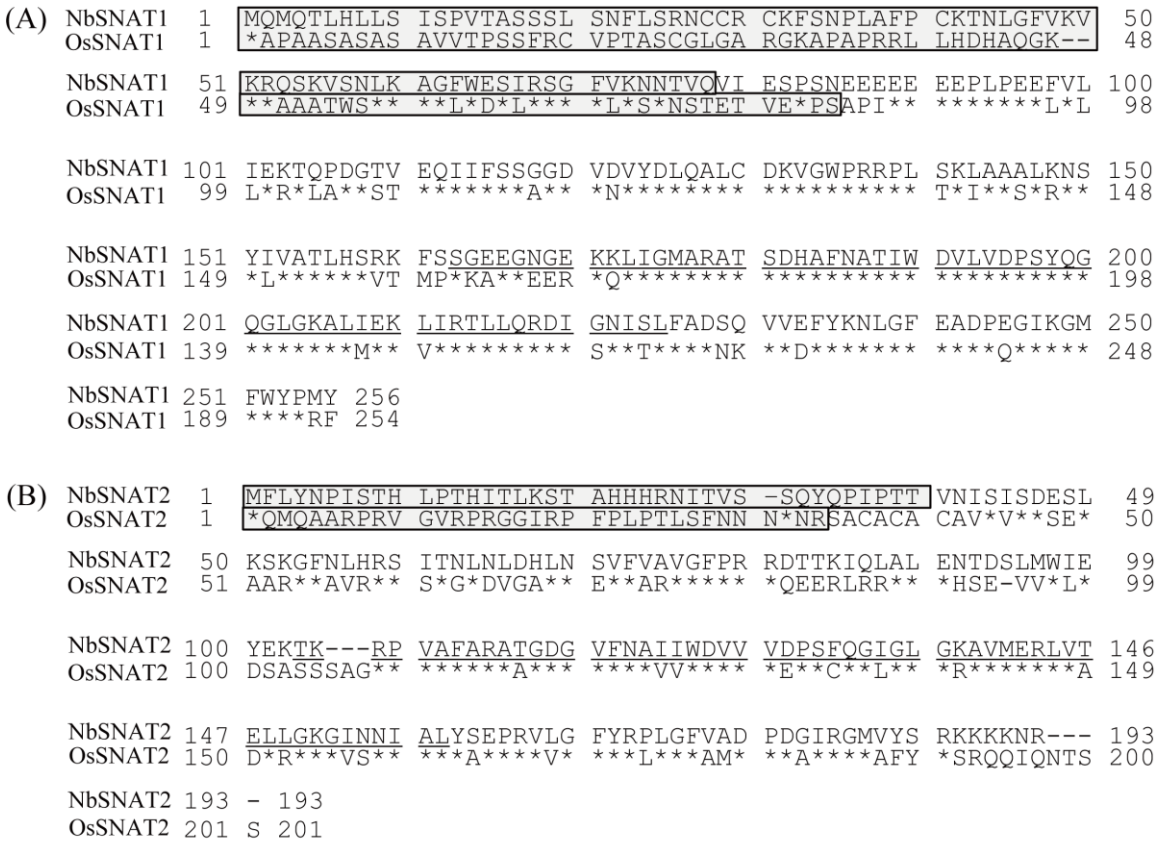

Fig. 1. Comparison of the predicted amino acid sequences of the serotonin *N*-acetyltransferase (*SNAT*) genes of tobacco and rice.

(A) Sequence comparison between rice SNAT1 (OsSNAT1) and tobacco SNAT1 (NbSNAT1). (B) Sequence comparison between rice SNAT2 (OsSNAT2) and tobacco SNAT2 (NbSNAT2). Identical amino acids are indicated by asterisks, and gaps are marked as dashes. Predicted chloroplast transit sequences are enclosed within boxes. Conserved acetyl-coenzyme A binding site motifs are underlined. The GenBank accession numbers of OsSNAT1, OsSNATY2, NbSNAT1, and NbSNAT2 are AK059369, AK068156, Niben101Scf09906g02025.1, and Niben101Scf10613g00009.1, respectively.

3.2. Heterologous expression and purification of NbSNAT proteins in *E. coli.*

To determine whether the two *NbSNAT* genes encode functional SNAT enzymes, we transformed expression vectors containing the *NbSNAT* genes into *E. coli* for functional expression and affinity purification. To express *NbSNAT1* and *NbSNAT2* in *E. coli*, the putative N-terminal transit sequences were removed from each gene (Figure 2A). The recombinant NbSNAT1 and NbSNAT2 proteins were purified by nickel ion affinity purification (Figure 2B). Purified recombinant NbSNAT1 proteins expressed from the pET300-Δ78NbSNAT1 and pET28-Δ78NbSNAT1 vectors exhibited similar SNAT enzyme activity levels, whereas recombinant NbSNAT2 expressed from the pET300-Δ39NbSNAT2 vector displayed no SNAT enzyme activity (Figure 2C).

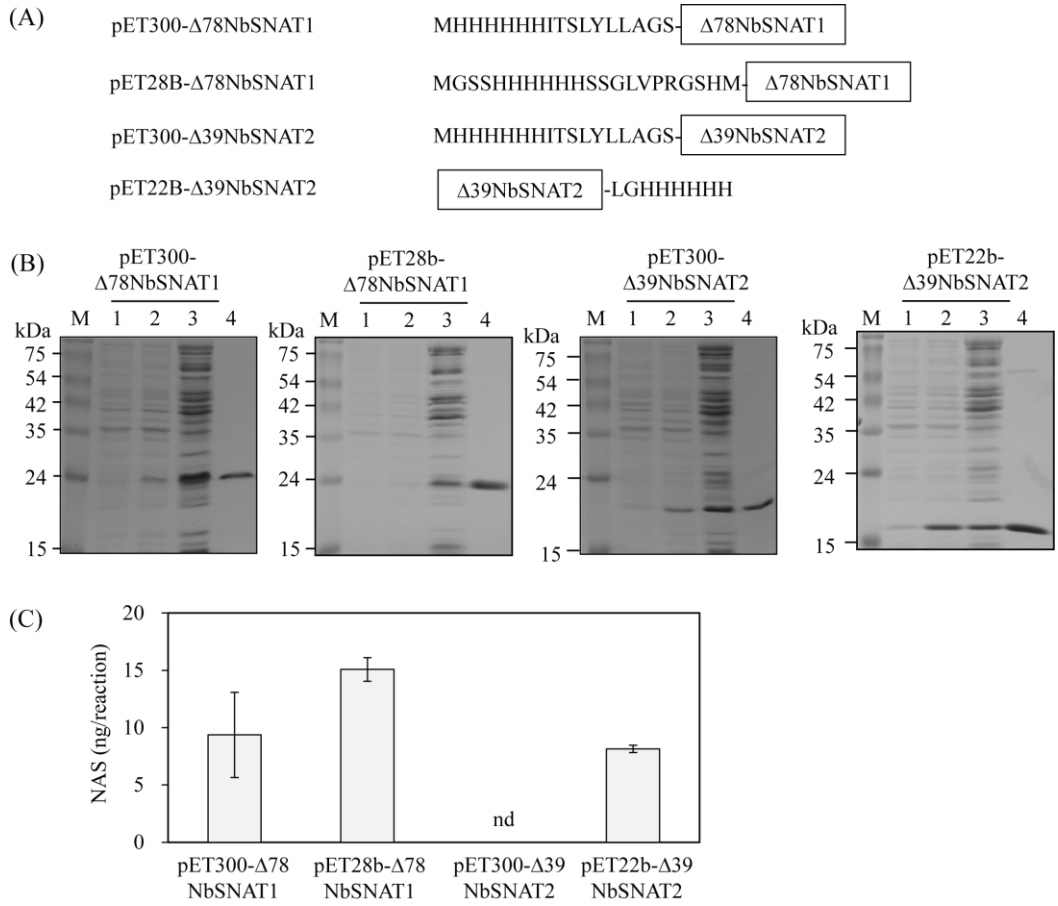

Fig. 2. Vector construction and purification of recombinant proteins.

(A) Schematic diagram of expression vectors harboring various forms of the NbSNAT genes ligated in-frame with DNA sequences coding for amino- or carboxy-terminal hexahistidine sequences. (B) Sodium dodecyl sulfate–polyacrylamide gel electrophoresis (SDS-PAGE) gels showing purified SNAT proteins. E. coli BL21(DE3) cultures harboring each plasmid construct were incubated with isopropyl ß-D-1-thiogalactopyranoside (IPTG) at 28°C for 5 h. Purified protein samples were separated by SDS-PAGE and stained for proteins using Coomassie blue. M, molecular mass standards; lane 1, total proteins in 10 µL aliquots of bacterial culture without IPTG; lane 2, total proteins in 10 µL aliquots of bacterial culture with IPTG; lane 3, 20 µg of soluble protein; lane 4, 5 µg of SNAT protein purified by affinity chromatography. nd, not determined. (C) Measurement of SNAT enzyme activity. NAS, N-Acetylserotonin. Data are represented as mean ± standard deviation of three independent replicates.

By contrast, recombinant NbSNAT2 expressed from the pET22b-Δ39NbSNAT2 plasmid exhibited functional SNAT enzyme activity, suggesting an inhibitory role of the N-terminal hexahistidine residues in the NbSNAT2 protein. Therefore, we selected vectors pET28-Δ78NbSNAT1 and pET22b-Δ39NbSNAT2 to produce recombinant NbSNAT1 and NbSNAT2, respectively, for further kinetic analyses.

3.3. Enzymatic features of recombinant NbSNAT1 and NbSNAT2 proteins.

Recombinant NbSNAT1 exhibited its highest SNAT activity at pH 8.8 and 45°C (Figure 3A, B). To determine the V_{max} and K_m of NbSNAT1, we applied a Lineweaver–Burk equation

using serotonin and 5-methoxytryptamine as substrates (Figure 3C); for serotonin, the K_m was 579 µM and the V_{max} was 136 pkat/mg protein, while the K_m was 945 µM and the V_{max} was 298 pkat/mg protein for 5-methoxytryptamine. The catalytic efficiencies (V_{max}/K_m) of NbSNAT1 for serotonin and 5-methoxytryptamine were 0.235 and 0.315, respectively.

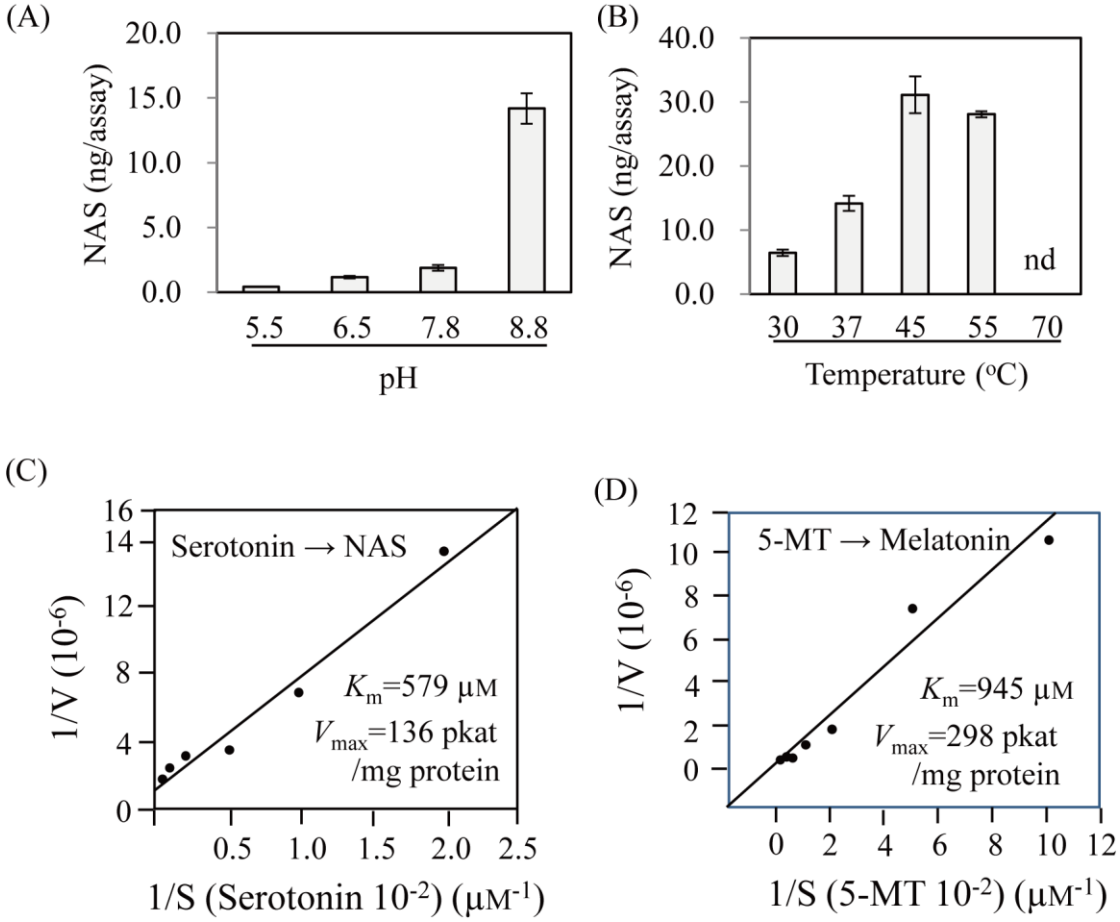

Fig. 3. Enzymatic characteristics of purified recombinant tobacco NbSNAT1.

SNAT enzyme activity as a function of (A) pH and (B) temperature. Determination of the substrate affinity (K_m) and maximum reaction rate (V_{max}) for serotonin (C) and 5-methoxytryptamine (D). NAS production catalyzed by purified NbSNAT1 protein (5 µg for A and B and C; 0.5 µg for C and D) was measured in vitro. Data are represented as mean ± standard deviation of three independent experiments. The V_{max} and K_m values were determined from Lineweaver–Burk plots. NAS, N-Acetylserotonin; nd, not determined; 5-MT, 5-methoxytryptamine.

Similar to NbSNAT1, the optimal conditions for NbSNAT2 were pH 8.8 and 45°C, respectively, (Figure 4A, B). However, unlike NbSNAT1, NbSNAT2 exhibited no SNAT enzyme activity at 55°C, indicating that NbSNAT2 was less tolerant to high temperatures than NbSNAT1. For NbSNAT2, the K_m values were 326 µM and 872 µM, and the V_{max} values were 26 pkat/mg and 92 pkat/mg, for serotonin and 5-methoxytryptamine, respectively. The V_{max}/K_m of NbSNAT2 for serotonin and 5-methoxytryptamine were 0.08 and 0.11, respectively. These results suggest that NbSNAT1 exhibited higher SNAT enzymic activity than NbSNAT2.

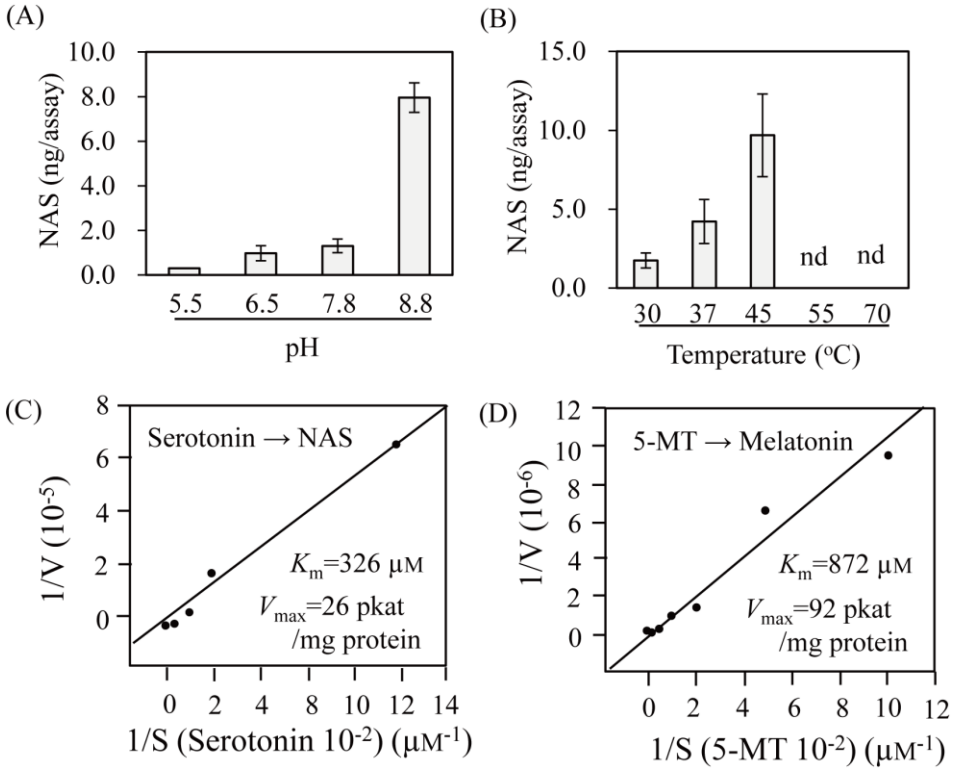

Fig. 4. Enzymatic characteristics of purified recombinant tobacco NbSNAT2.
SNAT enzyme activity as a function of (A) pH and (B) temperature, and the determination of V_{max} and K_m values for (C) serotonin and (D) 5-methoxytryptamine. NAS production catalyzed by purified NbSNAT2 protein (5 μg for A and B; 0.5 μg for C and D) was measured in vitro. Data represent the mean ± standard deviation of three independent experiments. The V_{max} and K_m values were determined using Lineweaver–Burk plots. NAS, N-Acetylserotonin ; nd, not determined; 5-MT, 5-methoxytryptamine.

In rice, melatonin inhibits OsSNAT activity via feedback inhibition (13). To determine whether this phenomenon also occurs in tobacco, we measured the activity of NbSNAT1 and NbSNAT2 under varying melatonin concentrations. NbSNAT1 activity was not inhibited by melatonin, suggesting a lack of melatonin-driven feedback inhibition (Figure 5). By contrast, NbSNAT2 activity increased at low melatonin concentrations (1 μM and 5 μM), while there was no significant difference in SNAT activity at higher (10 μM and 100 μM) melatonin concentrations compared to the 0 μM melatonin control. Our data suggest that neither NbSNAT1 nor NbSNAT2 exhibited feedback inhibition by melatonin, unlike OsSNAT2 (13).

3.4. Subcellular locations of NbSNAT1 and NbSNAT2.

We hypothesized that NbSNAT1 and NbSNAT2 would localize to chloroplasts due to their predicted N-terminal transit peptide sequences. To verify the subcellular locations of NbSNAT1 and NbSNAT2, we created two binary vector constructs containing *NbSNAT1* and *NbSNAT2* under the control of the estrogen-inducible XVE promoter. *Agrobacterium* cells harboring the vectors were applied to tobacco leaves, and the transformed leaves were examined using confocal microscopy. As shown in Figure 6, NbSANT1 and NbSNAT2 exhibited strong mCherry fluorescence, which co-localized with chlorophyll fluorescence. This indicated that NbSANT1 and NbSNAT2 localized to chloroplasts, which is consistent with SNAT proteins from other plant species (15, 17, 20, 26).

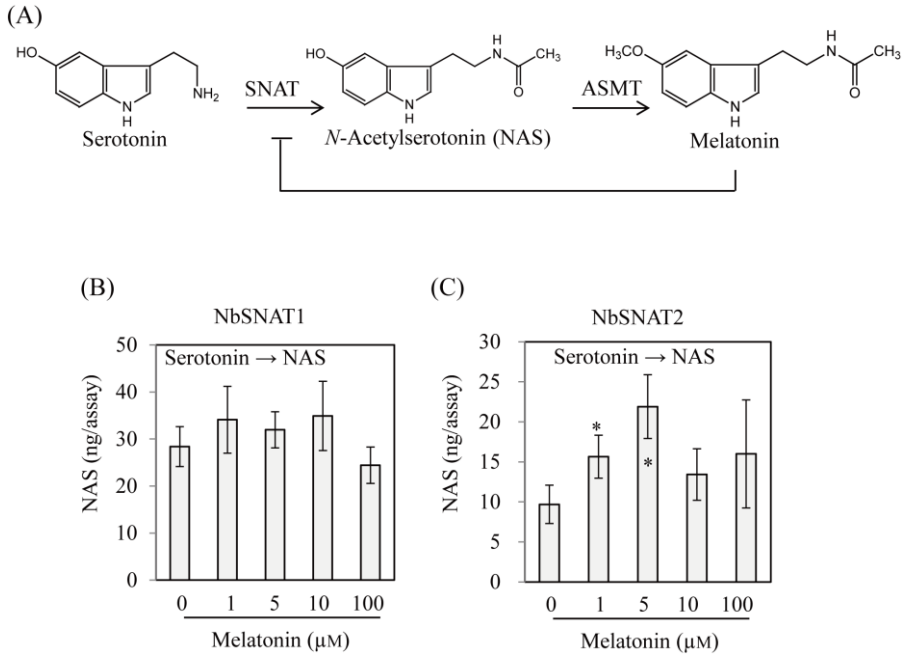

Fig. 5. Effects of melatonin on the SNAT enzyme activity of NbSNAT1 and NbSNAT2.

(A) Biosynthetic pathway of melatonin. (B, C) Feedback inhibition of NbSNAT enzymes by melatonin. Asterisks (*) indicate significant differences from the control as determined by Tukey's post-hoc honest significant difference test at P < 0.05. ASMT, N-acetylserotonin methyltransferase.

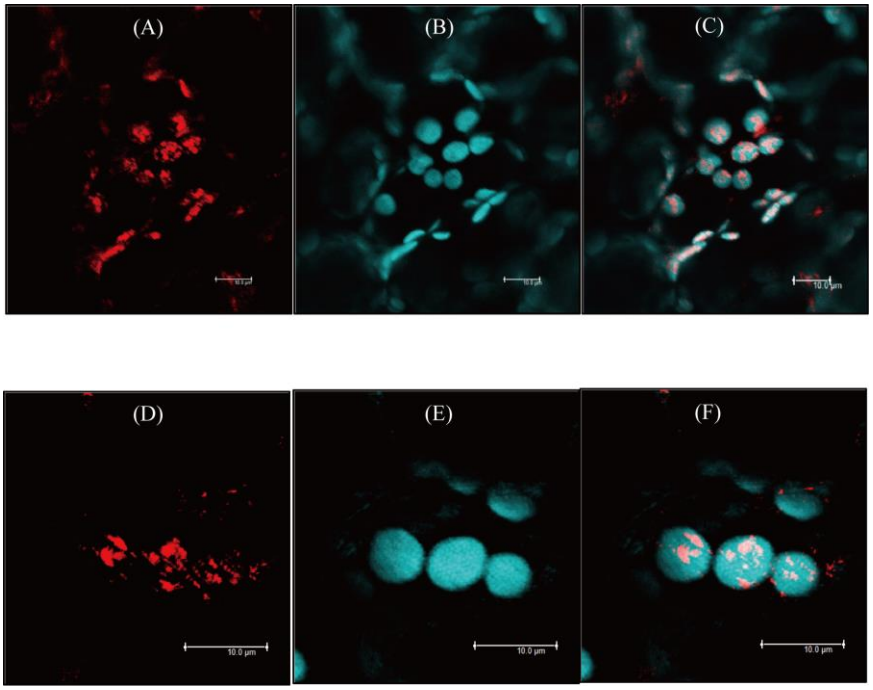

Fig. 6. Confocal microscopy analysis of NbSNAT1 and NbSNAT2 proteins.

(A) NbSNAT1-mCherry fluorescence (red), (B) chlorophyll fluorescence (cyan), (C) merged fluorescence of images (A) and (B), (D) NbSNAT2-mCherry fluorescence (red), (E) chlorophyll fluorescence (cyan), and (F) merged fluorescence of images (D) and (E). Thirty-day-old tobacco leaves were infiltrated with Agrobacterium tumefaciens strain GV2260 containing XVE-inducible NbSNAT-mCherry constructs. Scale bars = 10 μm.

3.5. Characteristics of transgenic tobacco plants overexpressing *NbSNAT1* or *NbSNAT2*.

A total of 13 independent T_0 transgenic tobacco plants overexpressing either *NbSNAT1* or *NbSNAT2* were initially generated (Figure 7). Most transgenic lines overexpressed *NbSNAT1* or *NbSNAT2*, with the exception of lines 1, 6, 11, and 12 of *NbSNAT1* and lines 3, 6, and 9–11 of *NbSNAT2*. After selfing the T_1 lines, T_2 homozygous lines of *NbSNAT1* or *NbSNAT2* were obtained for characterization.

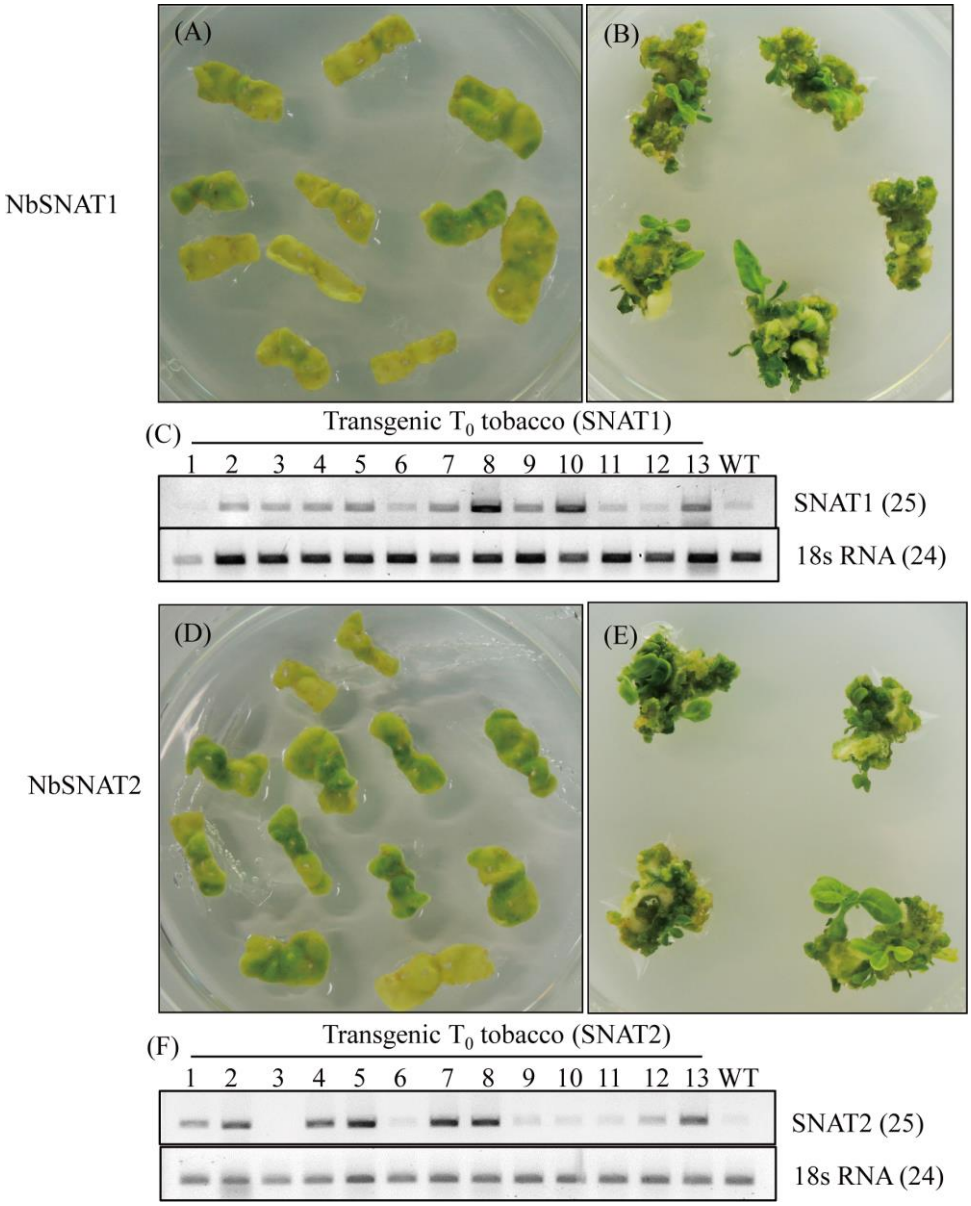

Fig. 7. Generation of transgenic tobacco plants.

(A) Leaf disk transformation and selection process of NbSNAT1 overexpression lines. (B) Shoot regeneration of transgenic tobacco overexpressing NbSNAT1. (C) Expression levels of NbSNAT1 mRNA measured by reverse transcription-polymerase chain reaction (RT-PCR) in T_0 transgenic tobacco plants transformed with NbSNAT1. (D) Leaf disk transformation and selection process of NbSNAT2 overexpression lines. (E) Shoot regeneration of transgenic tobacco overexpressing NbSNAT2. (F) Expression levels of NbSNAT2 mRNA measured by RT-PCR in T_0 transgenic tobacco plants expressing NbSNAT2. WT, wild type.

First, to determine whether the overexpression of *NbSNAT1* and *NbSNAT2* was associated with enhanced melatonin production, we quantified the melatonin contents of healthy tobacco leaves, as well as tobacco leaves challenged with 0.5 mM cadmium as an elicitor. As shown in Figure 8, the healthy leaves of both wild-type and transgenic tobacco produced 0.7 ng/g fresh weight (FW), indicating that melatonin was not overproduced in the *NbSNAT* overexpression lines. Moreover, when the leaves of wild-type and transgenic plants were treated with cadmium (0.5 mM), the melatonin levels increased to 0.9 ng/g FW in both the wild-type and transgenic lines (data not shown), suggesting that the overexpression of *NbSNAT* genes was not functionally linked to enhanced melatonin synthesis in tobacco. A similar phenomenon was also observed in transgenic rice overexpressing sheep *SNAT*, in which melatonin levels did not increase in the root tissues (27). The melatonin contents in *N. benthamiana* leaves with and without cadmium treatment were identical to those found in *N. tabacum* suspension cells (28).

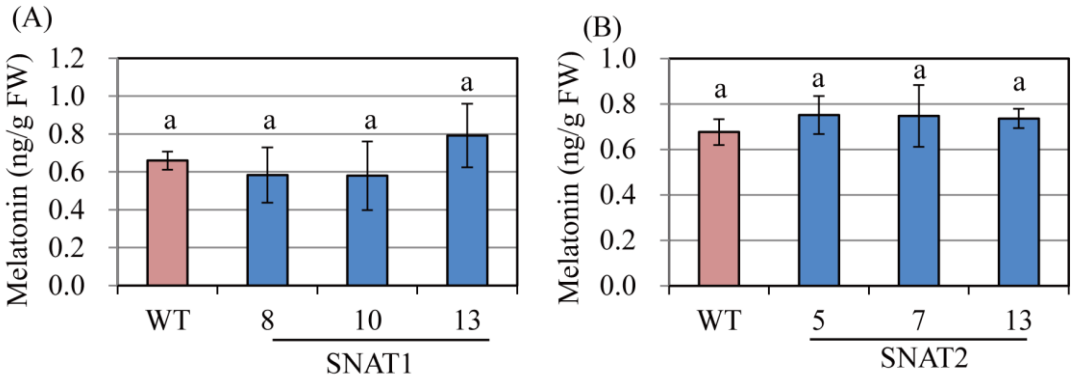

Fig. 8. Melatonin contents in tobacco transgenic plants either expressing *NbSNAT1* (A) or *NbSNAT2* (B).

Four-week-old tobacco leaves (T_2) were subjected to melatonin analysis. Different letters denote significant differences from the control as determined by Tukey's post-hoc honest significant difference test at $P < 0.05$.

4. DISCUSSION

Plant melatonin levels are highly variable among studies, which is potentially due to technical difficulties during melatonin extraction and a lack of precise quantification tools (29, 30). Contrary to earlier reports, recent measurements suggest that melatonin levels are relatively low in plant cells, ranging from picograms to a few nanograms per gram FW (5). Low plant melatonin levels are associated with reduced SNAT activity in plants compared to animals. For example, a purified recombinant sheep SNAT exhibited 9302 pkat/mg protein activity, whereas purified recombinant OsSNAT1 and OsSNAT2 showed 42 and 130 pkat/mg protein activity, respectively (13). Because SNAT is the penultimate enzyme in the melatonin biosynthetic pathway and is a rate-limiting enzyme in melatonin biosynthesis, SNAT enzyme activity directly affects the absolute levels of melatonin in plants. *SNAT* genes have been cloned from numerous plant species, including rice, pine, apple, arabidopsis, mulberry, and grapevine (5, 17); each of these SNAT enzymes exhibit similar enzyme kinetics, in terms of K_m and V_{max} values (Table 1). Despite tobacco being a dicotyledonous model plant that is easily transformable with a short life cycle and high seed production, no *SNAT* genes have been studied in tobacco until now.

NbSNAT1 and NbSNAT2 had K_m values for serotonin of 579 μM and 326 μM, and V_{max} values of 136 pkat/mg protein and 26 pkat/mg protein, respectively. These K_m and V_{max}

values were similar to those of other plants (Table 1). OsSNAT1 and OsSNAT2 have K_m values of 270 μM and 371 μM, and V_{max} values of 55 and 78 pkat/mg protein, respectively, for serotonin (31). The optimal temperatures of OsSNAT1 and OsSNAT2 were 55°C and 45°C, respectively, comparable to those of NbSNAT1 and NbSNAT2. Moreover, both NbSNAT1 and NbSNAT2 proteins localized to the chloroplasts, similar to OsSNAT enzymes (20). Typically, SNAT enzymes share similar kinetic features among plant species. However, NbSNAT2 was not feedback inhibited by melatonin (Figure 5), whereas rice and arabidopsis SNAT2 enzymes undergo significant melatonin-induced inhibition (13, 15).

Table 1. Substrate specificities of plant-related SNAT proteins.

Organism	Enzyme	K_m (μM)		Optimum temperature (^oC)	Reference
		Serotonin	5-MT		
Rice	SNAT1	270	nd	55	20
Rice	SNAT2	371	nd	45	13
Pine	SNAT1	428	nd	55	26
Arabidopsis	SNAT1	309	51	45	14
Arabidopsis	SNAT2	232	630	45-55	15
Grapevine	SNAT2	392	nd	45	17
Mulberry	SNAT1	163	68	nd	33
Apple	SNAT3	55	nd	35	34
Tobacco	SNAT1	579	945	55	This paper
Tobacco	SNAT2	326	872	45	This paper
Red algae	SNAT	467	nd	55	35
Cyanobacterium	SNAT	823	647	55	36

The functions of NbSNAT1 and NbSNAT2 were investigated by generating transgenic tobacco plants overexpressing either NbSNAT1 or NbSNAT2. Unfortunately, no clear melatonin overproduction was detected in the transgenic tobacco plants (Figure 8). *SNAT* gene overexpression does not always lead to increases in melatonin production in plants (27). This may be related to the rapid catabolism of either NAS or melatonin due to the activity of enzymes such as *N*-acetylserotonin deacetylase and melatonin 3-hydroxylase (5).

In this study, we cloned two *SNAT* isogenes from tobacco plants for the first time. The *SNAT* genes encoded enzymes that catalyze serotonin into NAS, the penultimate step in melatonin biosynthesis. We found that the recombinant tobacco SNAT proteins possessed SNAT enzyme activities, and that their enzyme kinetics were similar to those of other plants sharing identical key amino acid residues for SNAT activity (32). Given that *NbSNAT* overexpression did not lead to significant changes in melatonin levels in our study, future investigations involving the suppression of *NbSNAT* using RNA interference technology should be conducted in tobacco plants to further elucidate the role of melatonin during growth and development, as well as in response to adverse stimuli. More in-depth studies of NbSNAT will provide insight into the function of melatonin and its potential applications in improving the agronomic traits of tobacco plants.

ACKNOWLEDGEMENTS

This research was supported by Basic Research Program through the National Research Foundation of Korea (NRF) funded by the Ministry of Education (NRF-2021R1I1A2042237; NRF-2021R1C1C2006271), Republic of Korea

AUTHORSHIP

HYL and OJH performed the experiment; KB designed, wrote, and revised the manuscript.

CONFLICT OF INTEREST

The authors declare that the research was conducted in the absence of any commercial or financial relationship that could be construed as a potential conflict of interest.

REFERENCES

1. Hardeland R (2019) Melatonin in the evolution of plants and other phototrophs. *Melatonin Res*. **2**: 10-36.
2. Arnao MB, Hernández-Ruiz J (2021) Melatonin as a regulatory hub of plant hormone levels and action in stress situations. *Plant Biol*. **23**: 7-19.
3. Wang Y, Reiter RJ, Chan Z (2018) Phytomelatonin: a universal abiotic stress regulator. *J. Exp. Bot.* **69**: 963-974.
4. Arnao MB, Hernández-Ruiz J (2020) Melatonin in flowering, fruit set and fruit ripening. *Plant Reprod*. **33**: 77-87.
5. Back K (2021) Melatonin metabolism, signaling and possible roles in plants. *Plant J*. **105**: 376-391.
6. Lee HY, Back K (2018) Melatonin plays a pivotal role in conferring tolerance against endoplasmic reticulum stress via mitogen-activated protein kinases and bZIP60 in *Arabidopsis thaliana*. *Melatonin Res*. **1**: 93-107.
7. Lee HY, Back K (2021) Melatonin regulates chloroplast protein quality control via a mitogen-activated protein kinase signaling pathway. *Antioxidants* **10**: 511.
8. Hong Y, Zhang Y, Sinumporn S, Yu N, Zhan X, Shen X, Chen D, Yu P, Wu W, Liu Q, Cao Z, Zhao C, Cheng S, Cao L (2018) Premature leaf senescence 3, encoding a methyltransferase, is required for melatonin biosynthesis in rice. *Plant J.* **95**: 877-891.
9. Lu H, Luo T, Fu H, Wang L, Tan Y, Huang J, Wang Q, Ye G, Gatehouse AMR, Lou Y, Shu Q (2018) Resistance of rice to insect pests mediated by suppression of serotonin biosynthesis. *Nat. Plants* **4**: 338-344.
10. Zheng Y, Xu J, Wang F, Tang Y, Wei Z, Ji Z, Wang C, Zhao K (2021) Mutation types of CYP71P1 cause different phenotypes of mosaic spot lesion and premature leaf senescence in rice. *Front. Plant Sci*. **12**: 641300.
11. Dyda F, Klein DC, Hickman AB (2000) GCN5-related *N*-acetyltransferases: A structural overview. *Annu. Rev. Biophys. Biomol. Struct.* **29**: 81-103.
12. Kang K, Lee K, Park S, Byeon Y, Back K (2013) Molecular cloning of rice serotonin *N*-acetyltransferase, the penultimate gene in plant melatonin biosynthesis. *J. Pineal Res.* **55**: 7-13.
13. Byeon Y, Lee HY, Back K (2016) Cloning and characterization of the serotonin *N*-acetyltransferase-2 gene (*SNAT2*) in rice (*Oryza sativa*). *J. Pineal Res.* **61**: 198-207.
14. Lee HY, Byeon Y, Lee K, Lee HJ, Back K (2014) Cloning of *Arabidopsis* serotonin *N*-

acetyltransferase and its role with caffeic acid *O*-methyltransferase in the biosynthesis of melatonin in vitro despite their different subcellular localization. *J. Pineal Res.* **57**: 418-426.

15. Lee HY, Lee K, Back K (2019) Knockout of *Arabidopsis* serotonin *N*-acetyltransferase-2 reduces melatonin levels and delays flowering. *Biomolecules* **9**: 712.
16. Li C, He Q, Zhang F, Yu J, Li C, Zhao T, Zhang Y, Xie Q, Su B, Mei L, Zhu S, Chen J (2019) Melatonin enhances cotton immunity to *Verticillium* wilt via manipulating lignin and gossypol biosynthesis. *Plant J*. **100**: 784-800.
17. Yu Y, Bian L, Jiao Z, Keke Y, Wan Y, Zhang G, Guo D (2019) Molecular cloning and characterization of a grapevine (*Vitis vinifera* L.) serotonin *N*-acetyltransferase (*VvSNAT2*) gene involved in plant defense. *BMC Genomics* **20**: 880.
18. Wang X, Zhang H, Xie Q, Liu Y, Lv H, Bai R, Ma R, Li X, Zhang X, Guo YD, Zhang N (2020) SISNAT interacts with HSP40, a molecular chaperone, to regulate melatonin biosynthesis and promote thermotolerance in tomato. *Plant Cell Physiol.* **61**: 909-921.
19. Bombarely A, Rosli HG, Vrebalov J, Moffett P, Mueller LA, Martin GB (2012) A draft genome sequence of *Nicotiana benthamiana* to enhance molecular plant-microbe biology research. *Mol. Plant-Microbe Interact.* **25**: 1523-1530.
20. Byeon Y, Lee HY, Lee K, Park S, Back K (2014) Cellular localization and kinetics of the rice melatonin biosynthetic enzymes SNAT and ASMT. *J. Pineal Res.* **56**: 107-114.
21. Karimi M, Inze D, Depocker A (2002) Gateway vectors for Agrobacterium-mediated plant transformation. *Trends Plant Sci*. **7**: 193-195.
22. Duan W, Wang L, Song G (2016) *Agrobacterium tumefaciens*-mediated transformation of wild tobacco species *Nicotiana debneyi, Nicotiana clevelandii*, and *Nicotiana glutinosa*. *Am. J. Plant Sci*. **7**: 1-7.
23. Byeon Y, Back K (2016) Melatonin production in *Escherichia coli* by dual expression of serotonin *N*-acetyltransferase and caffeic acid *O*-methyltransferase. *Appl. Microbiol. Biotechnol*. **100**: 6683-6691.
24. Lee, HY, Back K (2020) The phytomelatonin receptor (PMRT1) *Arabidopsis* Cand2 is not a *bona fide* G protein-coupled melatonin receptor. *Melatonin Res*. **3**: 177-186.
25. Emanuelsson O, Nielsen H, Brunak S, Heijne G (2000) Predicting subcellular localization of proteins based on their N-terminal amino acid sequence. *J. Mol. Biol.* **300**: 1005-1016.
26. Park S, Byeon Y, Lee HY, Kim YS, Ahn T, Back K (2014) Cloning and characterization of a serotonin *N*-acetyltransferase from a gymnosperm, loblolly pine (*Pinus taeda*). *J. Pineal Res*. **57**: 348-355.
27. Park S, Back K (2012) Melatonin promotes seminal root elongation and root growth in transgenic rice after germination. *J. Pineal Res.* **53**: 385-389.
28. Kobylińska A, Reiter RJ, Posmyk MM (2017) Melatonin protects cultured tobacco cells against lead-induced cell death via inhibition of cytochrome C translocation. *Front. Plant Sci.* **8**: 1560.
29. Domingos ALG, Hermsdorff HHM, Bressan J (2019) Melatonin intake and potential chronobiological effects on human health. *Crit. Rev. Food Sci. Nutr.* **59**: 133-140.
30. Xu T, Chen Y, Kang H (2019) Melatonin is a potential target for improving post-harvest preservation of fruits and vegetables. *Front. Plant Sci*. **10**: 1388.
31. Back K, Tan DX, Reiter RJ (2016) Melatonin biosynthesis in plants: multiple pathways catalyze tryptophan to melatonin in the cytoplasm or chloroplasts. *J. Pineal Res.* **61**: 426-437.
32. Liao L, Zhou Y, Xu Y, Zhang Y, Liu X, Liu B, Chen X, Guo Y, Zeng Z, Zhao Y (2021) Structural and molecular dynamics analysis of plant serotonin *N*-acetyltransferase reveal an acid/base-assisted catalysis in melatonin biosynthesis. *Angew. Chem Int. Ed*. **60**: 12020-12026.

33. Zheng S, Zhu Y, Liu C, Fan W, Xiang Z, Zhao A (2021) Genome-wide identification and characterization of genes involved in melatonin biosynthesis in *Morus notabilis* (wild mulberry). Phytochemistry **189**: 112819.
34. Wang L, Feng C, Zheng X, Guo Y, Zhou F, Shan D, Liu X, Kong J (2017) Plant mitochondria synthesize melatonin and enhance the tolerance of plants to drought stress. *J. Pineal Res.* **63**: e12429.
35. Byeon Y, Lee HY, Choi DW, Back K (2015) Chloroplast encoded serotonin *N*-acetyltransferase in the red alga *Pyropia yezoensis*: gene transition to the nucleus from chloroplasts. *J. Exp. Bot.* **66**: 709-717.
36. Tan DX, Hardeland R, Back K, Manchester LC, Alatorre-Jimenez MA, Reiter RJ (2016) On the significance of an alternate pathway of melatonin synthesis via 5-methoxytryptamine: comparisons across species. *J. Pineal Res*. **61**: 27-40.

Please cite this paper as:
Back, K., Hyoung Yool, L. and Ok Jin, H. 2021. Functional characterization of tobacco (Nicotiana benthamiana) serotonin N-acetyltransferases (NbSNAT1 and NbSNAT2). Melatonin Research. 4, 4 (Dec. 2021), 507-521. DOI:https://doi.org/https://doi.org/10.32794/mr112500109.